AIAA JOURNAL
Vol. 31, No. 11, November 1993

Effect of Gain Length on Hydrogen Fluoride Chemical Laser Amplifier Performance

R. E. Waldo* and L. H. Sentman†
University of Illinois at Urbana-Champaign, Urbana, Illinois 61801

An amplifier performance model that predicts a device's amplifier performance given the device's oscillator performance as a function of reflectivity was developed. Excellent agreement between single pass model predictions and single pass experimental data was obtained. The model was used to predict amplifier performance as the gain length was scaled from 0.3 to 4 m for three different lasers. When the amplifier performance curve is plotted in terms of nondimensional powers ζ_{out} vs ζ_{in}, gain length dependent, device independent curves result. The nondimensional amplifier performance curve showed that, with a single pass amplifier, one 0.3-m oscillator may be able to drive three amplifiers and one 4-m oscillator might be able to drive eight amplifiers. These results, which are independent of device, are sensitive to the oscillator power vs reflectivity performance curve in the 0–20% reflectivity range.

Nomenclature

AR = amplification ratio, P_{out}/P_{in}
g = gain coefficient, cm^{-1}
g_0 = zero power or small signal gain coefficient, cm^{-1}
I = radiation flux, W/cm^2
I_s = saturation radiation flux, W/cm^2
L_e = thickness of the mixed flow ($=L_g$ when fully mixed)
L_g = geometric gain length
P_{in} = input power to the amplifier
$P_{out_{amp}}$ = P_{out}, output power from the amplifier
$P_{out_{osc}}$ = output power from the oscillator
R_{eff} = effective reflectivity of the oscillator's resonator reflectivity of the outcoupler mirror times the reflectivity of the feedback mirror
z = coordinate in the direction of the optical axis
α = nonsaturable distributed loss, cm^{-1}
Δ = $P_{out} - P_{in}$
δ = power/nozzle bank exit area, W/cm^2
ζ_{in} = nondimensional input power (input power to the amplifier/output power from the oscillator at $R_{eff} = 20\%$)
ζ_{out} = nondimensional output power (output power from the amplifier/output power from the oscillator at $R_{eff} = 20\%$)

I. Introduction

In Ref. 1, the performance of a continuous wave hydrogen fluoride (cw HF) chemical laser master oscillator with power amplifier was measured. The results of these measurements showed that, regardless of the oscillator or resonator used to generate the input beam, the amplification ratio is an inverse function of the input power (intensity); and, for maximum amplification, the peak of the input intensity distribution must be matched to the peak of the zero power gain distribution in the amplifier. The measured P_{out} vs P_{in} performance curve showed that, after a rapid increase, the difference $P_{out} - P_{in}$ increased slowly over a wide range of input powers. These data showed that between one-third and one-half of the device's oscillator output must be input to obtain amplifier output equal to the device's oscillator performance.

To determine the extent to which these subscale experiments apply to large-scale devices, an analytical model that predicts a device's amplifier performance given the device's oscillator performance as a function of reflectivity was developed.[2,3] The computer simulations of two subsonic arc driven [University of Illinois at Urbana-Champaign (UIUC) CL II and Helios CL II] and one supersonic combustion driven (CL XI) cw HF lasers were used to predict their oscillator performance as a function of reflectivity and gain length L_g. The computer simulations were performed with Blaze II,[4] a chemical laser simulation program that was baselined to the experimental oscillator data for each laser at a fixed value of L_g. The oscillator power vs reflectivity was calculated for reflectivities from 0.001 to 99.9% and gain lengths from 0.30 to 4.0 m. These oscillator performance curves were then used in the amplifier model to predict amplifier performance, P_{out} vs P_{in} and AR vs P_{in}, as L_g was scaled to 4 m.

The amplifier performance model is introduced in Sec. II. Section III compares the experimental and calculated amplifier performance of the UIUC CL II laser. The calculated oscillator performance as a function of L_g for three different devices is presented in Sec. IV. Section V contains the corresponding amplifier performance. Implications for master oscillator/power amplifier (MOPA) performance are discussed in Sec. VI. Several concluding remarks are given in Sec. VII.

II. Analytical Model for Amplifier Performance

An analytical model that predicts a device's amplifier performance given the device's oscillator performance (output power) as a function of reflectivity was developed. The model is based on the observation[2,3] that the response of the gain medium is independent of the source of the radiative flux to which the medium is exposed; thus, the average gain in the amplifier is the same as the saturated gain in the oscillator when the circulating radiative flux in the oscillator is the same as the average radiative flux in the amplifier. This approach to model amplifier performance differs from that of traditional amplifier theory.

Existing amplifier models[5-8] calculate amplifier performance using a modified version of Beer's Law,

$$\frac{dI(z)}{dz} = I(z)\{g[I(z)] - \alpha\} \tag{1}$$

Received Nov. 12, 1991; revision received March 4, 1993; accepted for publication March 8, 1993.

*Research Assistant, Aeronautical and Astronautical Engineering Department; currently Research Scientist, W. J. Schafer Associates, Inc., 26565 W. Agoura Road, Suite 202, Calabases, CA 91302. Member AIAA.

†Professor, Aeronautical and Astronautical Engineering Department. Associate Fellow AIAA.

where $I(z)$ is the radiation flux (W/cm^2), a function of z (cm), the distance in the direction of propagation of radiation through the amplifier; $g[I(z)]$ is the gain coefficient (cm^{-1}) in the laser's cavity, a function of $I(z)$ and, therefore, z; and α is a nonsaturable distributed loss (cm^{-1}). For a laser with homogeneous line broadening, when the gain decreases proportionately over the entire transition line, the gain coefficient g decreases with intensity $I(z)$ according to the relation[5]

$$g(z) = g_0/[1 + I(z)/I_s] \tag{2}$$

To predict amplifier and oscillator performance with this approach, the three quantities g_0, α, and I_s must be known. As discussed in Ref. 8, these quantities cannot be completely determined from oscillator performance data alone. Amplifier performance data are also required. These parameters are varied until a good match between model and measurements are obtained.

The advantage of the present model is that it permits the calculation of amplifier performance from a knowledge of oscillator performance only. Since this information is normally available from experiments or computer simulations, the present model allows the estimation of a device's amplifier performance with a simple calculation. The present model takes advantage of the fact that information about the details of a device's performance (gain, nonsaturable distributed loss, saturation intensity, etc.), whether operated as an oscillator or an amplifier, is contained in the device's oscillator performance. It calculates a device's amplifier performance directly from the same device's oscillator performance as a function of reflectivity. This model gives amplifier performance (P_{out} and AR) in an easy straightforward way without requiring knowledge of the details of the device's performance.

The present model is based on the observation that the average gain in the amplifier will be the same as the saturated gain in the oscillator when the circulating radiative flux in the oscillator is the same as the average radiative flux in the amplifier. The circulating radiative flux in the oscillator is defined by

$$P_{\text{cir}_{\text{osc}}} = \frac{P_{\text{out}_{\text{osc}}}}{1 - R_{\text{eff}}} \tag{3}$$

An approximation of the average radiative flux in the amplifier is given by

$$P_{\text{av}_{\text{amp}}} = \tfrac{1}{2}(P_{\text{in}_{\text{amp}}} + P_{\text{out}_{\text{amp}}}) \tag{4}$$

The circulating radiative flux in the oscillator is set equal to the average radiative flux in the amplifier to yield

$$\frac{P_{\text{out}_{\text{osc}}}}{1 - R_{\text{eff}}} = \tfrac{1}{2}(P_{\text{in}_{\text{amp}}} + P_{\text{out}_{\text{amp}}}) \tag{5}$$

When Eq. (5) is satisfied, the average gain in the amplifier

$$\alpha_{\text{amp}} = \frac{1}{L_e} \ln\left(\frac{P_{\text{out}_{\text{amp}}}}{P_{\text{in}_{\text{amp}}}}\right) \tag{6}$$

is set equal to the saturated gain in the oscillator

$$\alpha_{\text{sat}} = -\frac{1}{2L_e} \ln (R_{\text{eff}}) \tag{7}$$

which gives

$$P_{\text{out}_{\text{amp}}} = P_{\text{in}_{\text{amp}}}\left(\frac{1}{\sqrt{R_{\text{eff}}}}\right) \tag{8}$$

Substitution of Eq. (8) into Eq. (5) gives

$$\frac{P_{\text{out}_{\text{osc}}}}{1 - R_{\text{eff}}} = \frac{P_{\text{in}_{\text{amp}}}}{2}\left(1 + \frac{1}{\sqrt{R_{\text{eff}}}}\right) \tag{9}$$

If the oscillator performance $P_{\text{out}_{\text{osc}}}$ is expressed as a function of R_{eff}, Eq. (9) becomes an equation for R_{eff} in terms of $P_{\text{in}_{\text{amp}}}$. The experimental oscillator power $P_{\text{out}_{\text{osc}}}$ can be approximated with a linear function of R_{eff}, i.e.,

$$P_{\text{out}_{\text{osc}}} = F(R_{\text{eff}}) = aR_{\text{eff}} + b \tag{10}$$

where a and b are constant over a range of R_{eff}. The a and b for each range of R_{eff} are determined from the device's oscillator performance curve. It is observed that an oscillator performance curve can be accurately represented by three or four straight line segments. This is based on the fact that oscillator performance curves[2] are linear for R_{eff} between 0.2 and 0.8 (20 and 80%). Substitution of Eq. (10) into Eq. (9) yields an equation for R_{eff} in terms of $P_{\text{in}_{\text{amp}}}$

$$(P_{\text{in}_{\text{amp}}} + 2a)R_{\text{eff}}^{3/2} + P_{\text{in}_{\text{amp}}}R_{\text{eff}} + (2b - P_{\text{in}_{\text{amp}}})R_{\text{eff}}^{1/2} - P_{\text{in}_{\text{amp}}} = 0 \tag{11}$$

Given a $P_{\text{in}_{\text{amp}}}$, this equation is solved for R_{eff}. The given $P_{\text{in}_{\text{amp}}}$ and corresponding R_{eff} are then substituted into Eq. (8) to calculate the device's amplifier performance $P_{\text{out}_{\text{amp}}}$ as a function of $P_{\text{in}_{\text{amp}}}$.

III. Evaluation of the Amplifier Performance Model

To determine how well the model predicts amplifier performance, the UIUC CL II experimental oscillator performance data are used as input to the model. Figure 1 shows the UIUC CL II experimental oscillator power vs reflectivity data for run 36 flow rates. From Fig. 1 it is seen that the output power is linear for reflectivities (R_{eff}) between 0.2 (20%) and 0.8 (80%) and begins to decrease for R_{eff} above 80%. It was shown analytically[9] that this decrease of output power is caused by nonsaturable distributed losses in the lasing cavity and/or mirror absorption/scattering losses.

Figure 1 shows straightline approximations of the data. Segments 2 ($0.2 \le R_{\text{eff}} \le 0.8$), 5 ($0.8 \le R_{\text{eff}} \le 0.93$) and 6 ($0.93 \le R_{\text{eff}} \le 0.999$) were chosen to agree with the data. Since there are no oscillator data for $0 \le R_{\text{eff}} \le 0.2$ and the oscillator output power must go to zero at $R_{\text{eff}} = 0$, the oscillator performance for $0 \le R_{\text{eff}} \le 0.2$ was approximated by a straight line, segment 1. Segments 3 ($0.8 \le R_{\text{eff}} \le 0.99$) and 4 ($0.99 \le R_{\text{eff}} \le 0.999$) were calculated by Blaze II,[4] a two-dimensional, rotational equilibrium, finite rate, chemical kinetic, mixing laser simulation code. The Blaze II calculations did not include any losses and yielded a maximum oscillator output power[9] of 117.02 W at $R_{\text{eff}} = 0.999$. Since segments 3 and 4 do not include any losses, they provide an upper bound on amplifier performance for the range of $R_{\text{eff}} \ge 0.8$; however, it will be shown in the following discussion that the amplifier's performance corresponding to this range of R_{eff} is of little interest.

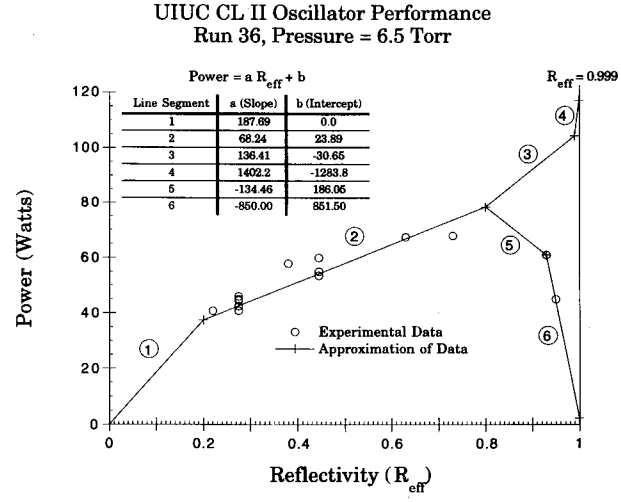

Fig. 1 Straight line approximations to the power vs reflectivity curve for the UIUC CL II laser for run 36 flow rates.

The two approximations of the CL II oscillator power vs reflectivity for run 36 flow rates, segments 1, 2, 3, and 4 (case A) and segments 1, 2, 5, and 6 (case B), Fig. 1, were used to calculate P_{out} for the run 36 flow rates in the amplifier as a function of P_{in}, Tables 1 (case A) and 2 (case B). These results are compared to the run 36 flow rates amplifier data,[1-3] Figs. 2 and 3. From Fig. 2 and Table 1, it is seen that there is very good agreement between the model and experimental data and that Δ ($\Delta = P_{out} - P_{in}$) increases slowly over a wide range of P_{in}, increasing from a value of 35.85 W at $P_{in} = 29.0$ W to a maximum of 58.53 W at $P_{in} = 116{,}968.54$ W. The Δ of 58.53 W is one-half of the maximum oscillator output power of 117.02 W predicted by Blaze II at an R_{eff} of 99.9%. This suggests that, in the limit, an amplifier can only extract half of the energy from a gain cell that an oscillator can extract from the same gain cell. This result is a surprise because in the high intensity limit, the amplifier should completely saturate the gain medium, and if both the amplifier gain medium and oscillator gain medium are completely saturated, it seems that the same energy should be extracted from each. Since no data are available to confirm the amplifier model calculations at the high intensity limit, these results should be considered qualitative.

Figure 3 shows that there is no difference between case A and case B until a P_{in} of 370.52 W is reached which corresponds to $R_{eff} = 80\%$. This is the P_{in} at which the model either follows segments 3 and 4 (case A) or segments 5 and 6 (case B). These calculations show the rapid increase of Δ at low P_{in}. When the amplifier does not have nonsaturable distributed losses in the lasing cavity, case A, the energy removed from

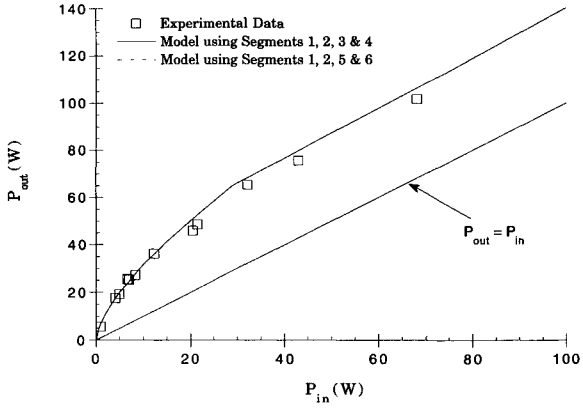

Fig. 2 UIUC CL II amplifier performance for run 36 flow rates as a function of input power; experimental data and model predictions plotted for input powers of 0–100 W yielding identical prediction of amplifier performance for segments 1, 2, 3, and 4 and for 1, 2, 5, and 6.

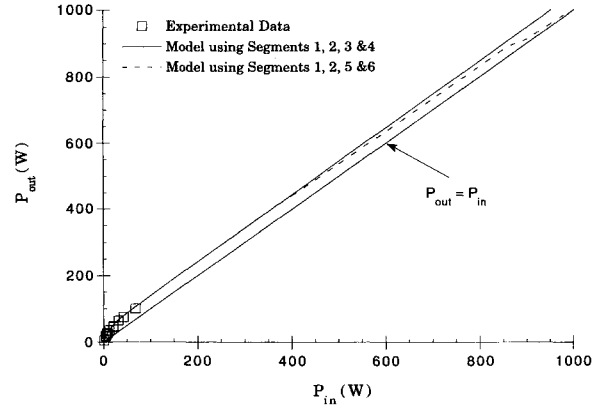

Fig. 3 UIUC CL II amplifier performance for run 36 flow rates as a function of input power; experimental data and model predictions plotted for input powers of 0–1000 W.

Table 1 Amplifier model predictions of output power, amplification ratio, and $\Delta = P_{out} - P_{in}$ as a function of input power for run 36 flow rates in the amplifier[a]

P_{in}, W	R_{eff}	P_{out}, W	AR	Δ, W
0.0	0.000	0.00	0.00	0.00
1.0	0.021	7.06	7.06	6.06
2.0	0.033	10.99	5.50	8.99
3.0	0.044	14.32	4.77	11.32
4.0	0.054	17.29	4.32	13.29
5.0	0.062	20.02	4.00	15.02
10.0	0.100	31.65	3.17	21.65
15.0	0.131	41.48	2.77	26.48
20.0	0.158	50.35	2.52	30.35
29.0	0.200	64.85	2.24	35.85
40.0	0.272	76.68	1.92	36.68
50.0	0.327	87.41	1.75	37.41
100.0	0.511	139.96	1.40	39.96
150.0	0.614	191.37	1.28	41.37
200.0	0.682	242.25	1.21	42.25
250.0	0.729	292.85	1.171	42.85
300.0	0.764	343.29	1.144	43.29
350.0	0.791	393.62	1.125	43.62
370.5	0.800	414.26	1.118	43.74
400.0	0.811	444.27	1.111	44.27
450.0	0.826	495.04	1.100	45.04
500.0	0.840	545.68	1.091	45.68
550.0	0.851	596.23	1.084	46.23
600.0	0.861	646.70	1.078	46.70
700.0	0.877	747.46	1.068	47.46
800.0	0.890	848.05	1.060	48.05
900.0	0.900	948.53	1.054	48.53
1,000.0	0.909	1,048.92	1.049	48.92
5,000.0	0.980	5,052.02	1.010	52.02
10,413.36	0.990	10,465.82	1.005	52.46
116,968.54	0.999	117,027.07	1.001	58.53

[a]Calculations use segments 1-4 shown in Fig. 1.

Table 2 Amplifier model predictions of output power, amplification ratio, and $\Delta = P_{out} - P_{in}$ as a function of input power for run 36 flow rates in the amplifier[a]

P_{in}, W	R_{eff}	P_{out}, W	AR	Δ, W
0.0	0.000	0.00	0.00	0.00
1.0	0.021	7.06	7.06	6.06
2.0	0.033	10.99	5.50	8.99
3.0	0.044	14.32	4.77	11.32
4.0	0.054	17.29	4.32	13.29
5.0	0.062	20.02	4.00	15.02
10.0	0.100	31.65	3.17	21.65
15.0	0.131	41.48	2.77	26.48
20.0	0.158	50.35	2.52	30.35
29.0	0.200	64.85	2.24	35.85
40.0	0.272	76.68	1.92	36.68
50.0	0.327	87.41	1.75	37.41
100.0	0.511	139.96	1.40	39.96
150.0	0.614	191.37	1.28	41.37
200.0	0.682	242.25	1.21	42.25
250.0	0.729	292.85	1.171	42.85
300.0	0.764	343.29	1.144	43.29
350.0	0.791	393.62	1.125	43.62
370.5	0.800	414.26	1.118	43.74
400.0	0.820	441.76	1.104	41.76
450.0	0.846	489.23	1.087	39.23
500.0	0.866	537.38	1.075	37.38
550.0	0.881	585.97	1.065	35.97
600.0	0.893	634.86	1.058	34.86
700.0	0.911	733.24	1.047	33.24
855.7	0.930	887.28	1.037	31.58
900.0	0.973	912.27	1.014	12.27
1000.0	0.990	1004.96	1.005	4.96
2349.41	0.999	2350.59	1.001	1.18

[a]Calculations use segments 1, 2, 5, and 6 shown in Fig. 1.

the amplifier reaches its maximum value at very large P_{in}. However, when the amplifier does have nonsaturable distributed losses in the lasing cavity, case B, the energy removed from the amplifier reaches some maximum value (less than case A) and then decreases to zero as P_{in} continues to increase.

The reason for this behavior is that at low P_{in} the energy extraction from the amplifier increases exponentially with P_{in} which results in a rapid increase in Δ. As P_{in} gets larger, the Δ increases more slowly because the amplifier's gain media begins to saturate. If an amplifier has nonsaturable distributed loss, at small P_{in}, the energy lost is small compared to the energy extracted from the amplifier. However, at large P_{in}, the energy lost can equal the energy extracted from the amplifier resulting in Δ approaching zero as P_{in} increases to large values.

The CL II oscillator performance[2] at run 36 flow rates with a 20% reflective outcoupler is 36 and 68 W with a 73% reflective outcoupler. Figure 2 shows that to obtain a total power of 36 W after the amplifier, about 12 W must be input; and to obtain 68 W after the amplifier, about 34 W must be input. These data show that between one-third and one-half of the device's oscillator output must be input to obtain amplifier output equal to the device's oscillator performance when the oscillator is operated with a 20 and 73% reflective outcoupler, respectively. Based on these considerations, the P_{in} of interest will be 34 W or less, which from Table 1 is seen to correspond to $R_{eff} < 25\%$. Since the oscillator data show that the nonsaturable distributed losses do not become important until R_{eff} is greater than 80%, the nonsaturable distributed losses do not play a significant role in predicting the CL II amplifier performance. Thus, the details of the oscillator performance curve for R_{eff} greater than 25% do not affect the amplifier performance in the range of P_{in} of interest. This demonstrates the importance of the oscillator performance for $R_{eff} < 25\%$ in predicting amplifier performance for P_{in} of interest. These conclusions, based on results obtained for the UIUC CL II laser, are shown to be valid for other devices in the following sections.

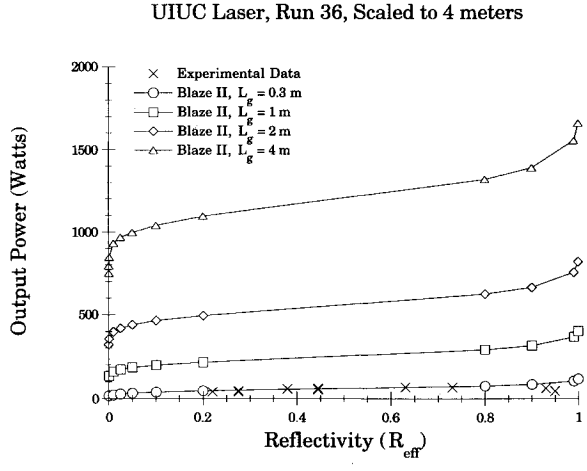

Fig. 4 Power vs reflectivity for the UIUC laser for run 36 flow rates when scaled to large values of L_g.

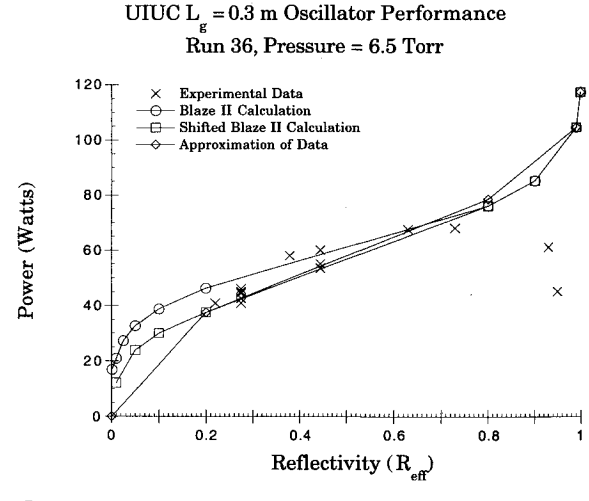

Fig. 5 Experimental and calculated power vs reflectivity for the UIUC CL II laser for run 36 flow rates.

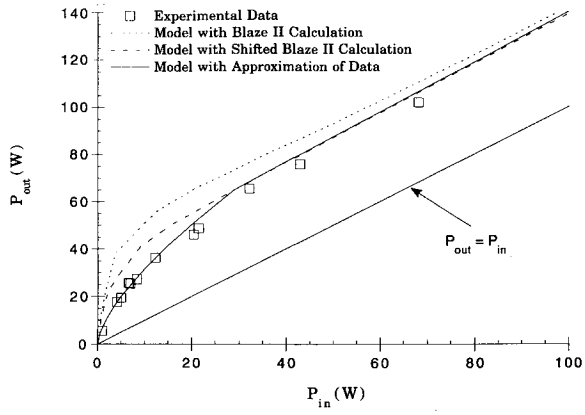

Fig. 6 Experimental and calculated UIUC CL II amplifier performance for run 36 flow rates as a function of input power.

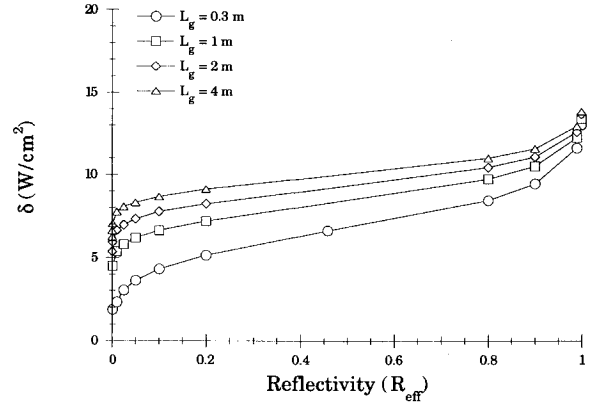

Fig. 7 Power per nozzle bank exit area δ vs reflectivity for the UIUC laser for run 36 flow rates when scaled to large values of L_g; height of nozzle bank held fixed as L_g increased.

IV. Oscillator Performance as a Function of Gain Length

To determine amplifier performance as a function of gain length, the oscillator performance as a function of gain length must be known. The Blaze II laser simulation code was separately baselined to the UIUC[2] and Helios[10] 0.3-m lasers and was used to predict the performance of these lasers for gain lengths of 0.3, 1, 2, and 4 m over a range of mirror reflectivities from 0.001 to 99.9%. (In Ref. 10, the Blaze II code, anchored to a Helios 15-cm laser, successfully predicted the performance of a Helios 75-cm laser. These results provide confidence in the capability of Blaze II to scale laser performance.) The calculations were performed assuming that the laser did not have a nonsaturable distributed loss and that the mirrors have zero absorption/scattering losses as discussed in Sec. III. The calculated oscillator performance curves for the UIUC laser are shown in Fig. 4. These figures show how the output power of the laser increases as the gain length is scaled from 0.3 to 4 m. Before examining the effect of L_g on oscillator performance, the Blaze II oscillator calculation and the experimental oscillator data for the UIUC 0.3-m laser are compared and used to predict amplifier performance.

Figure 5 shows the same experimental data and Blaze II calculation shown in Fig. 4 for the 0.3-m case on an expanded

scale. From Fig. 5 it is seen that the Blaze II calculation generally agrees with the data but is high for $R_{\text{eff}} \leq 50\%$. To make the Blaze II calculation agree with the data over the entire range of R_{eff}, all of the Blaze II data points for $R_{\text{eff}} \leq 20\%$ were shifted down by 8.8 W. The resulting curve is denoted as Shifted Blaze II Calculation, Fig. 5. This shifted curve agrees much better with the data, and it agrees well with the Approximation of Data curve (the same approximation of data curve shown in Fig. 1) except for the range of $R_{\text{eff}} < 20\%$. Since there are no oscillator data for $R_{\text{eff}} < 20\%$, it is impossible to determine what the oscillator performance is in this range; however, the shifted Blaze II calculation is an attempt to use a detailed laser simulation model, anchored to data, to predict the oscillator performance in this range.

Amplifier performance was calculated using all of the three curves shown in Fig. 5 and compared to amplifier data in Fig. 6. Figure 6 shows the significant change in amplifier performance that results from a change in oscillator performance. In particular, the large differences in the amplifier performance for $P_{\text{in}} < 30$ W (the range of interest, Sec. III) is a direct result of the difference between the oscillator performance curves from $R_{\text{eff}} = 0$ to 20%. This large difference in amplifier performance changes the number of amplifiers one oscillator can drive. To obtain a total power of 36 W after the amplifier, about 12 W must be input with the approximation of data curve but only about 7 W with the shifted Blaze II calculation. This comparison shows that one oscillator can drive between 3 and 5 amplifiers depending on which curve is followed. This again demonstrates that for the UIUC CL II laser, the oscillator performance for $R_{\text{eff}} \leq 20\%$ must be known so that amplifier performance in the range of interest can be calculated accurately. The fact that the model with approximation of data curve in Fig. 6 matches the amplifier data very well suggests that the approximation of data curve in Fig. 5 is an accurate representation of the oscillator performance.

To clearly show the effect of L_g on oscillator performance, Fig. 4 is replotted as δ (power per nozzle bank exit area) vs R_{eff} in Fig. 7. Three points are made from this figure. First, in the limit of $R_{\text{eff}} \rightarrow 1$, the δ for a given device approaches the same value independent of L_g. This demonstrates that to extract all of the available energy from a gain cell, the gain medium must be driven very hard, and that when all of the energy is extracted from a gain cell, the output power from the gain cell will scale linearly with L_g, a physically reasonable result.

The second point is that the value of R_{eff} at which the δ vs R_{eff} curve first becomes linear with R_{eff} (the break point) decreases with increasing L_g. Earlier in this section it was shown that, for the UIUC 0.3-m laser, the power vs reflectivity curve was linear over the ranges $0.0 \leq R_{\text{eff}} \leq 0.2$ and $0.2 \leq R_{\text{eff}} \leq 0.8$ (the break point occurred at $R_{\text{eff}} = 0.2$) and

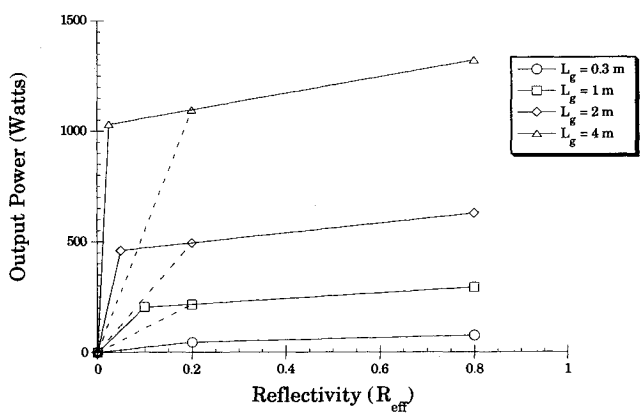

Fig. 8 Straight line approximations to the oscillator performance of the UIUC laser for run 36 flow rates when scaled to large values of L_g: ——, oscillator performance when oscillator break points are a function of L_g; ------, oscillator performance when oscillator break points occur at $R_{\text{eff}} = 20\%$ for all L_g.

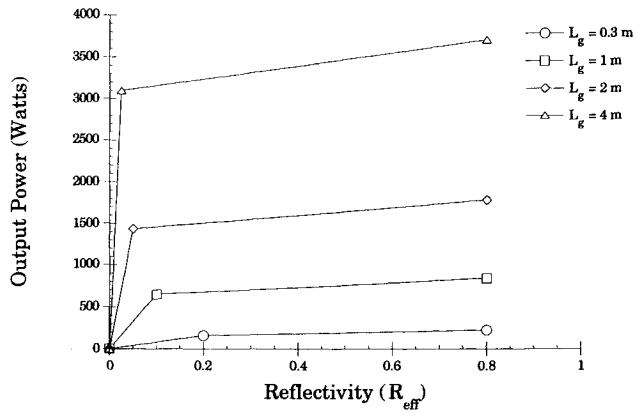

Fig. 9 Straight line approximations to the oscillator performance of the Helios laser when scaled to large values of L_g.

that the shifted Blaze II calculation overpredicted the amplifier performance for $R_{\text{eff}} \leq 0.2$. With this knowledge and Fig. 7, it is seen that the break point can be chosen to occur at a value of R_{eff} of 0.2 for the 0.3-m laser, 0.1 for the 1-m laser, 0.05 for the 2-m laser, and 0.025 for the 4-m laser. Since the value used for this break point has a significant effect when these oscillator curves are used to predict amplifier performance in the next section, the amplifier performance for the UIUC laser will also be calculated with oscillator performance curves that break at an $R_{\text{eff}} = 20\%$ for all four L_g. This should provide a lower bound estimate for the UIUC amplifier performance and demonstrate the importance of the location of the break point on amplifier performance.

The final point to be made from Fig. 7 is that the slope of the oscillator curve between the break point and $R_{\text{eff}} = 80\%$ decreases with increasing gain length. This suggests that the percentage of the available power that can be extracted from an oscillator at a fixed value of reflectivity increases with L_g. This is analytically expressed by Eq. (7) which shows that α_{sat} decreases (increasing power extraction) with increasing L_g (or L_e) at a fixed value of reflectivity.

V. Amplifier Performance Versus Gain Length

The oscillator performance curves generated in Sec. IV were used to calculate the devices' amplifier performance. The form of the oscillator performance curves used as input to the amplifier performance model to calculate each device's amplifier performance, P_{out} vs P_{in}, as a function of gain length are shown in Figs. 8 and 9. Figure 8 shows the straight line approximation of the Blaze II oscillator performance calculations for the UIUC laser when the break point is a function of L_g and when the break point is chosen to occur at $R_{\text{eff}} = 20\%$ for the four different L_g. Figure 9 is the straight line approximation of the Blaze II oscillator performance calculations for the Helios laser.

To better understand how gain length affects amplifier performance, it would be useful if a nondimensional parameter could be found which would collapse all of these curves to one device independent performance curve. Since scale effects are contained in the device's oscillator performance, a possible nondimensional parameter could come from dividing the amplifier performance, P_{out} vs P_{in}, by the device's oscillator performance. The P_{out} vs P_{in} amplifier performance of the UIUC laser and the Helios laser is plotted as ζ_{out} vs ζ_{in} in Figs. 10–12 for L_g of 0.3, 1, 2, and 4 m. The ζ_{out} and ζ_{in} are nondimensional powers given by

$$\zeta_{\text{out}} = \frac{P_{\text{out}}}{P_{\text{out}_{\text{osc}}}(R_{\text{eff}} = 20\%)} \tag{12}$$

$$\zeta_{\text{in}} = \frac{P_{\text{in}}}{P_{\text{out}_{\text{osc}}}(R_{\text{eff}} = 20\%)} \tag{13}$$

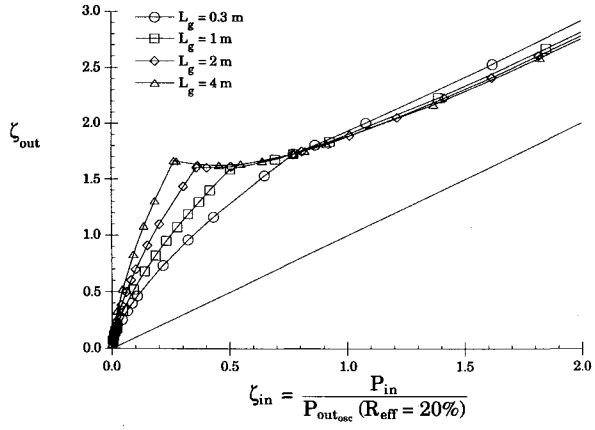

Fig. 10 Amplifier performance, ζ_{out} vs ζ_{in}, for the UIUC laser as a function of L_g for run 36 flow rates; curves calculated with the oscillator break point a function of L_g.

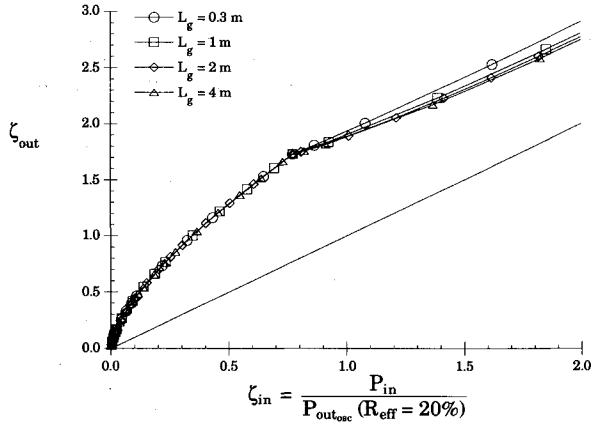

Fig. 11 Amplifier performance, ζ_{out} vs ζ_{in}, for the UIUC laser as a function of L_g for run 36 flow rates; curves calculated with the oscillator break point at $R_{eff} = 20\%$ for all L_g.

The P_{out} and P_{in} were nondimensionalized with the devices' oscillator performance with a 20% reflective outcoupler, $R_{eff} = 20\%$ (the value of R_{eff} used to select the reference value of $P_{out_{osc}}$ is arbitrary as long as the same value of R_{eff} is used for all gain lengths and devices).

The nondimensional curves in Figs. 10–12 clearly show the effects of L_g and break point on amplifier performance. It is seen for the UIUC laser that, when the break point is gain length independent (occurs at the same value of R_{eff} for all L_g), the ζ_{out} vs ζ_{in} curves, Fig. 11, for different L_g reduce to one curve. When the break point is L_g dependent, the ζ_{out} vs ζ_{in} curves, Fig. 10, for different L_g have an L_g dependence for small ζ_{in}. Comparison of Figs. 10 and 12 shows that, when the break point for a fixed L_g is independent of device, the ζ_{out} vs ζ_{in} curves are independent of device. This is further demonstrated in Fig. 13 which shows for three different devices, all with $L_g = 4$ m, that one ζ_{out} vs ζ_{in} curve results independent of device when the break point is independent of device for a fixed L_g. Finally, comparison of Figs. 10–12 shows that, when the break point is at the same R_{eff}, independent of L_g and device, one curve results independent of gain length and device.

The ζ_{out} vs ζ_{in} curves are used to determine how many amplifiers one oscillator can drive if the amplifier output power must be equal to the output power of the device when operated as an oscillator. Since the ζ_{out} vs ζ_{in} curves were nondimensionalized with the devices' oscillator performance with a 20% reflective outcoupler, the value of ζ_{in} at which the amplifier performance curve first reaches a value of $\zeta_{out} = 1$ determines the number of amplifiers one oscillator can drive when the oscillator is operated with a 20% reflective outcoupler.

From Fig. 11 it is seen that, for $\zeta_{out} = 1$ (amplifier performance equal to the device's oscillator performance), ζ_{in} must be 0.34 which means that one oscillator can drive at most three ($1/\zeta_{in}$) amplifiers if the amplifiers are to produce as much power as could be obtained by running them as oscillators. This result is independent of gain length and device when the oscillator performance break point occurs at the same value of R_{eff} for the different gain lengths and devices.

Figures 10 and 12 both show that when the break point varies with gain length, the number of amplifiers an oscillator can drive is gain length dependent. The number of amplifiers an oscillator can drive as a function of gain length is shown in Fig. 14. Figure 14 shows that, with a 4-m gain length, one oscillator may be able to drive as many as eight amplifiers; this result, however, depends on the shape of the oscillator performance curve for $R_{eff} \leq 20\%$.

VI. Master Oscillator/Power Amplifier Performance

The amplifier performance curves presented in the previous section are now used to investigate several MOPA design criteria, i.e., input power, output power, and the number of amplifiers. No attempt will be made to design a MOPA system due to the complexity of the problem. Instead, the amplifier performance curves are used to examine the performance of a typical MOPA system in which the output from one oscillator is divided evenly and injected into N amplifiers, and the output beams are added. The beams can be added incoherently or coherently. Since this calculation was done in terms of powers, the results are independent of how the beams are combined (a practical system calculation would be done in terms of inten-

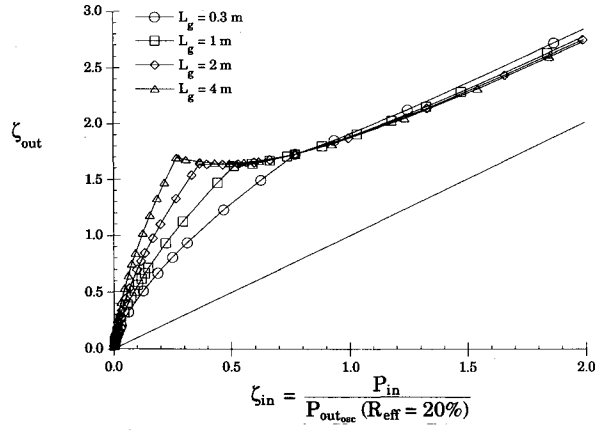

Fig. 12 Amplifier performance, ζ_{out} vs ζ_{in}, for the Helios laser as a function of L_g; curves calculated with the oscillator break point a function of L_g.

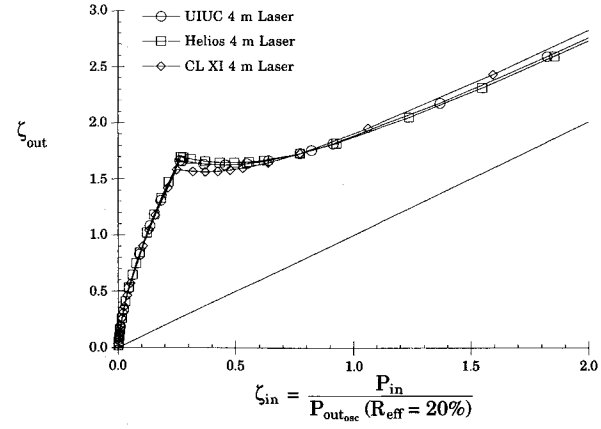

Fig. 13 Amplifier performance, ζ_{out} vs ζ_{in}, for three different lasers with $L_g = 4$ m.

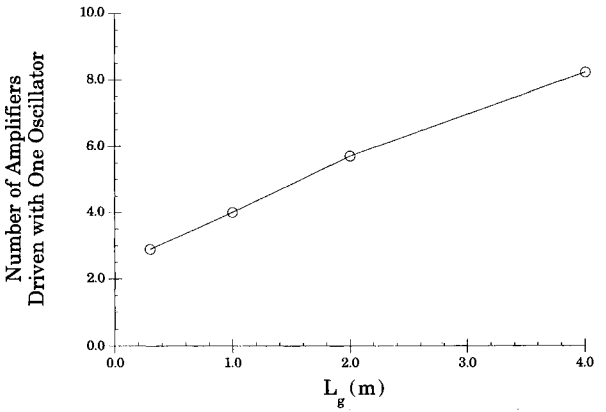

Fig. 14 Number of amplifiers one oscillator can drive and obtain amplifier performance equal to the performance that could be obtained by running the device as an oscillator as a function of L_g.

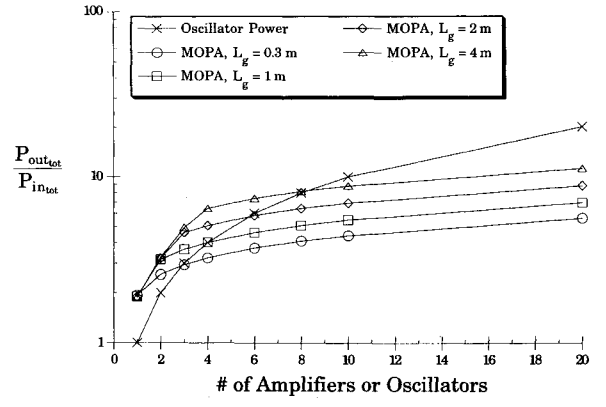

Fig. 15 Comparison of 0.3-, 1-, 2-, and 4-m MOPA performance with the performance of the same number of oscillators; note: master oscillator in the MOPA system not counted, i.e., the total number of devices is "# of Amplifiers" + 1.

sity in which case phase matching of the beams would be an important consideration to obtain maximum intensity when the multiple beams were combined). The results of the MOPA calculation are compared with the addition of N oscillators where the oscillators and amplifiers are all separate devices of the same type. The amplifier model presented in Sec. II was used to perform all the calculations, the MOPA systems were assumed to possess no losses, and the total output powers for the MOPA systems were calculated by adding the individual output powers from each amplifier.

The oscillator performance curves for the UIUC laser when the break point is a function of L_g, shown in Fig. 8, were used to calculate the MOPA performance for the UIUC laser for gain lengths of 0.3, 1, 2, and 4 m. Figure 15 is a plot of $P_{\text{out}_{\text{tot}}}/P_{\text{in}_{\text{tot}}}$ (the sum of the output powers of all the devices, amplifiers or oscillators, divided by the output power of the master oscillator) as a function of the number of amplifiers driven by the master oscillator. The x represent the total power obtained from a given number of oscillators. The other symbols represent the corresponding total power obtained from the same number of devices when they are operated as amplifiers with gain lengths of 0.3, 1, 2, and 4 m.

Three points can be made from Fig. 15. First, when comparing x points to other points, it is evident that a system of multiple oscillators outperforms a MOPA system when the MOPA system exceeds the number of amplifiers that can be driven by one oscillator. Second, the MOPA curves in Fig. 15 show that MOPA performance increases with increasing L_g. This is a result of the fact that a higher percentage of the amplifier's available energy can be extracted for a fixed P_{in} as the L_g of the amplifier increases. The analogous argument was presented for the oscillator in Sec. IV. Third, the curves shown in Fig. 15 are device independent because it was shown in the last section that the amplifier performance for a given gain length is independent of device if the break point occurs at the same R_{eff} for all devices. As a result of this observation, if any two of the three design criteria of a 0.3-, 1-, 2-, or 4-m MOPA system, i.e., input power, output power, or number of amplifiers, are specified, the third can be obtained from Fig. 15, independent of device.

The oscillator performance curves for the UIUC laser when the break point is chosen to occur at $R_{\text{eff}} = 20\%$ for the four different L_g, shown in Fig. 8, were used to calculate the MOPA performance for the UIUC laser for gain lengths of 0.3, 1, 2, and 4 m. Since it was shown in the last section that the amplifier performance calculated with these curves is independent of device and gain length, Fig. 11, the calculated MOPA performance is also independent of device and gain length. This MOPA performance is the same as that shown in Fig. 15 for the 0.3-m device, independent of device and gain length. This is a direct result of the break point occurring at the same value of R_{eff} independent of device and gain length.

VII. Concluding Remarks

An analytical model that predicts a device's amplifier performance given the device's oscillator performance as a function of reflectivity was developed. The model is based on the observation that the response of the gain medium is independent of the source of the radiative flux to which the medium is exposed; thus, the average gain in the amplifier is the same as the saturated gain in the oscillator when the circulating radiative flux in the oscillator is the same as the average radiative flux in the amplifier. Excellent agreement between model predictions and experimental data was obtained.

Oscillator performance (power vs R_{eff}) curves were generated for three different lasers for gain lengths of 0.3, 1, 2, and 4 m. These curves show, independent of device, that in the limit $R_{\text{eff}} \to 1$ the δ for a given device approaches the same value independent of L_g and that the value of R_{eff} at which the δ vs R_{eff} curve first becomes linear with R_{eff} (the break point) decreases with increasing L_g.

The amplifier model used these oscillator performance curves to calculate the devices' amplifier performance as gain length was scaled to 4 m. These calculations showed that in the oscillator performance in the range $0 \leq R_{\text{eff}} \leq$ the break point determines the amplifier performance in the range of interest. When the amplifier performance is plotted as ζ_{out} vs ζ_{in}, gain length dependent, device independent curves result. These curves show that with a 4-m gain length, if the amplifiers are to produce as much power as could be obtained by running them as oscillators, one oscillator may be able to drive as many as eight amplifiers.

The performance of a typical MOPA system was compared with the corresponding performance of the same number of oscillators. The MOPA had a slight performance advantage over the combined oscillators when the number of devices was less than or equal to the number of amplifiers an oscillator can drive and obtain amplifier performance that is equal to what could be obtained by running the devices as oscillators. When the number of devices was larger than this, the combined oscillators outperformed the MOPA.

Acknowledgments

This work was supported by the Strategic Defense Initiative Organization through W. J. Schafer Associates Subcontract SC-88K-33-004 and by the University of Illinois.

References

[1]Sentman, L. H., Waldo, R. E., Theodoropoulos, P. T., Nguyen, T. X., and Carroll, D. L., "Hydrogen Fluoride Chemical Laser Amplifier Performance: Experiment," *AIAA Journal*, Vol. 30, No. 1, 1992, pp. 138–144.

[2]Sentman, L. H., Waldo, R., Nguyen, T., and Theodoropoulos, P., "cw HF Chemical Laser Oscillator/Amplifier Performance in a

MOPA Configuration," Aeronautical and Astronautical Engineering Dept., Univ. of Illinois, TR 88-7, UILU Eng 88-0507, Urbana, IL, July 1988.

[3]Waldo, R. E., Sentman, L. H., Theodoropoulos, P. T., and Carroll, D. L., "On the Performance Characteristics of Multiple Pass HF Chemical Laser Master Oscillator/Power Amplifiers," Aeronautical and Astronautical Engineering Dept., Univ. of Illinois, TR 91-6, UILU Eng 91-0506, Urbana, IL, Aug. 1991.

[4]Sentman, L. H., Subbiah, M., and Zelazny, S. W., "BLAZE II, a Chemical Laser Simulation Program," Bell Aerospace Textron, TR H-CR-77-8, Buffalo, NY, Feb. 1977.

[5]Rigrod, W. W., "Gain Saturation and Output Power of Optical Masers," *Journal of Applied Physics,* Vol. 34, No. 9, 1963, pp. 2602–2609.

[6]Rigrod, W. W., "Saturation Effects in High Gain Lasers," *Journal of Applied Physics,* Vol. 36, No. 8, 1965, pp. 2487–2490.

[7]Rigrod, W. W., "Homogeneously Broadened CW Lasers with Uniform Distributed Loss," *IEEE Journal of Quantum Electronics,* Vol. QE-14, No. 5, 1978, pp. 377–381.

[8]Rice, J. K., Tisone, G. C., and Patterson, E. L., "Oscillator Performance and Energy Extraction from a KrF Laser Pumped by a High-Intensity Relativistic Electron Beam," *IEEE Journal of Quantum Electronics,* Vol. QE-16, No. 12, 1980, pp. 1315–1325.

[9]Emanuel, G., "Analytical Model for a Continuous Chemical Laser," *Journal of Quantative Spectroscopy and Radiative Transfer,* Vol. 11, No. 11, 1971, pp. 1481–1520.

[10]Sentman, L. H., "Performance Scaling of Oscillating Amplifiers," Aeronautical and Astronautical Engineering Dept., Univ. of Illinois, Final Rept. AAE TR 88-4, UILU Eng 88-0504, Urbana, IL, April 1988.